Inorg. Chem. **2003**, *42*, 4215–4222

Zeolite-Mediated Photochemical Charge Separation Using a Surface-Entrapped Ruthenium–Polypyridyl Complex

Yanghee Kim, Hyunjung Lee, and Prabir K. Dutta*

Department of Chemistry, The Ohio State University, 120 W 18th Avenue, Columbus, Ohio 43210

Amitava Das

Central Salt and Marne Chemicals Research Institute, Bhavnagar 364002, Gujarat, India

Received February 26, 2003

Employing the strategy of quaternization of the 2,2′ N atoms of the conjugated bipyridine ligand 1,4-bis[2-(4′-methyl-2,2′-bipyrid-4-yl)ethenyl]benzene (L), a polypyridyl complex of ruthenium(II) was tethered on the surface of zeolite Y. Electrochemical and spectroscopic properties of the complex suggest that, upon visible photoexcitation of the MLCT band, the electron is localized on the conjugated ligand rather than the bipyridines. Electron transfer from the surface complex to bipyridinium ions (methyl viologen) within the zeolite was observed. Visible light photolysis of the ruthenium–zeolite solid ion-exchanged with diquat and suspended in a propyl viologen sulfonate solution led to permanent formation of the blue propyl viologen sulfonate radical ion in solution. The model that is proposed involves intrazeolitic charge transfer to ion-exchanged diquat followed by interfacial (zeolite to solution) electron transfer to propyl viologen sulfonate in solution. Because of the slow intramolecular back-electron-transfer reaction and the forward electron propagation via the ion-exchanged diquat, Ru(III) is formed. This Ru(III) complex formed on the zeolite is proposed to react rapidly with water in the presence of light, followed by reaction with the propyl viologen sulfonate, to form pyridones and regeneration of Ru(II), which then continues the photochemical process.

Introduction

Natural photosynthesis involves the conversion of solar energy to chemicals via a complex array of light-harvesting pigments and redox species arranged spatially across membranes.[1] If systems that mimic photosynthesis can be designed, sunlight reaching the earth's surface can be exploited to generate chemicals.[2] To construct an efficient energy conversion system, it is necessary to create long-lived accessible photogenerated charge-separated species. The thermal back-electron-transfer reaction makes this difficult; e.g., with the photosensitizer tris(bipyridine)ruthenium-(II) ($Ru(bpy)_3^{2+}$) and the electron acceptor methyl viologen (MV^{2+}), the forward- and back-electron-transfer rate constants are reported to be 5.6×10^9 and 2.4×10^9 M^{-1} s^{-1}, respectively.[3]

Heterogeneous supports including micelles,[4] vesicles,[5] silica gel,[6] clays,[7] and zeolites[8] have been examined as supports for the $Ru(bpy)_3^{2+}$ and viologen system. Zeolite-based systems have shown promise for generation of long-lived charge-separated species. Using dyad molecules exchanged on the surface of zeolites, the intramolecular back-electron-transfer reactions between $Ru(bpy)_3^{3+}$ and viologen radical were found to be 10^5 times slower than in solution.[9] Several groups have shown that the back electron transfer between zeolite-entrapped $Ru(bpy)_3^{3+}$ and viologen radical

* To whom correspondence should be addressed. E-mail: dutta.1@osu.edu. Phone: 614-292-4532. Fax: 614-688-5402.

(1) Lawlor, D. W. *Photosynthesis: Molecular, Physiological, and Environmental Processes*, 2nd ed.; Longman: Essex, U.K., 1993.
(2) Parmon, V. N.; Zamarev, K. I. *Photocatalysis: Fundamentals and Applications*; Serpone, N., Pelizetti, E., Eds.; Wiley: New York, 1989; pp 565−602.
(3) Kalyanasundaram, K. *Coord. Chem. Rev.* **1982**, *46*, 159−244.
(4) Kunjappu, J. T.; Somasundaran, P.; Turro, N. J. *J. Phys. Chem*. **1990**, *94*, 8464.
(5) Lanne, C.; Ford, W. E.; Otvos, J. W.; Calvin, M. *Proc. Natl. Acad. Sci. U.S.A.* **1981**, *78*, 2017.
(6) Castellano, F. N.; Meyer, G. J. *J. Phys. Chem*. **1995**, *99*, 14742.
(7) Colon, J. L.; Yang, C.; Clearfild, A.; Martin, C. R. *J. Phys. Chem.* **1990**, *94*, 874.
(8) Vaidyalingam, A. S.; Coutant, M. A.; Dutta, P. K *Electron-Transfer In Chemistry*; Balzani, V., Ed.; Wiley-VCH: Weinheim, Germany, 2001; Vol. 4, pp 412−486.
(9) Yonemoto, E. H.; Kim, Y. I.; Schmehl, R. H.; Wallin, J. O.; Shoulders, B. A.; Richardson, B. R.; Haw, J. F.; Mallouk, T. E. *J. Am. Chem. Soc*. **1994**, *116*, 10557.

10.1021/ic034216o CCC: $25.00
Published on Web 06/06/2003

can be slowed, and charge hopping between intrazeolitic viologen molecules can lead to permanent photoinduced charge separation.[10−13] However, in these latter cases, Ru(bpy)$_3^{2+}$ was within the zeolite and not accessible for possible chemical utilization.

In this study, we address the accessibility problem by examining a system in which a polypyridine−ruthenium moiety is covalently bonded to entrapped bipyridinium acceptors on the surface of the zeolite. Previous studies of polypyridylruthenium complexes on surface of zeolite Y have included surface ion exchange of Ru(bpy)$_3^{2+}$ and (bpy)$_2$RuX^{n+}, where X includes a viologen moiety connected via saturated spacers to the coordinated bpy on the ruthenium, and have focused primarily on dynamics of photoelectron transfer.[9,14,15]

Several groups have reported synthesis of bpy-based ligands which are part of a conjugated unit.[16,17] The lifetimes of the polypyridylruthenium complexes with such conjugated ligands tend to be longer and are attractive for charge separation studies, although the price of conjugation is the decrease in excited-state redox potential.[17] In this paper, we have focused on such a ligand, 1,4-bis[2-(4′-methyl-2,2′-bipyrid-4-yl)ethenyl] benzene (L) first reported by Schmehl and co-workers.[16] By quaternizing the part of the ligand that is held in the zeolite, it has been possible to anchor the ruthenium complex on the surface of the zeolite. Charge transport from the photosensitizer on the zeolite to acceptors in solution via electron propagation through the bipyridinium-loaded zeolite is examined.

Experimental Section

A. Chemicals. Zeolite Y (LZY-52) from Union Carbide was ion-exchanged with 2 M NaCl solutions and calcined at 500 °C to remove impurities. Tetrahydrofuran (THF), acetonitrile, diisopropynamine, and *n*-hexane were dried and distilled before use. Ru(bpy)$_3^{2+}$ (Strem Chemicals), (bpy)$_2$RuCl$_2$ (Strem chemicals), 4,4′-dimethyl-2,2′-bipyridine (dmb, Aldrich), 1,4-dibromobutane (Aldrich), terephthaldehyde (Aldrich), $POCl_3$ (Aldrich), AIBN (Lancaster), and methyl viologen dichloride hydrate (MV^{2+}, Aldrich) were used as received. *N*-Bromosuccinimide (NBS, Aldrich) was recrystallized prior to use. Lithium diisopropylamide (LDA) was prepared in situ from equimolar amounts of *n*-butyllithium (Aldrich) and diisopropylamine (Aldrich) in dry THF. *N*,*N*′-Tetramethyl-2,2′-bipyridinium dibromide (4DQ^{2+}) and propyl viologen sulfonate (PVS) were synthesized by following reported procedures.[18] All reactions were carried out in an anaerobic atmosphere.

B. Synthesis. 1,4-Bis[2-(4′-methyl-2,2′-bipyrid-4-yl)ethenyl]-benzene (L). Ligand L was prepared according to the literature method with slight modifications.[16] To a THF solution of dmb (3.685 g, 20 mmol), maintained at 0 °C, a THF solution of LDA (20 mmol) was added dropwise, and the new solution was allowed to stir for 1 h. To this solution terephthalaldehyde (1.314 g, 10 mmol, in THF) was added in a dropwise manner. The resultant reaction mixture was allowed to attain room temperature and stirred overnight. Then the reaction was quenched with a few drops of water. After evaporation of organic solvent under reduced pressure, intermediate diol was extracted in chloroform layer. This was dried, and the crude product was recrystallized from ethanol. This purified diol intermediate was dissolved in ∼25 mL of dry pyridine and cooled to ∼5 °C. To this solution was added a pyridine solution of phosphoryl chloride (1.86 mL, 20 mmol), maintaining the reaction temperature at around 5 °C. The resulting reaction mixture was stirred at room temperature for 2 h. The unreacted $POCl_3$ was quenched with water, and reaction mixture was evaporated to dryness in vacuo. The crude product was dissolved in 1.0 M HCl solution, and the undesired organic compounds were removed by solvent extraction ($CHCl_3$). The pH of the aqueous solution was adjusted to ∼5.5 with NaOH solution, and the desired product was extracted in $CHCl_3$ layer. This was dried and purified by column chromatography using alumina (grade III) as stationary phase and CH_2Cl_2–CH_3OH (98.5:1.5; v/v) as eluent. ^{1}H NMR ($CDCl_3$): δ 8.65 (d, J = 5.1 Hz, 2H), 8.58 (d, J = 5.0 Hz, 2H), 8.54 (s, 2H), 8.27(s, 2H), 7.60 (s, 4H), 7.47 (d, J = 16.3 Hz, 2H), 7.39 (d−d, J = 5.1, 1.6 Hz, 2H), 7.17(d, J = 16.3 Hz, 2H), 7.19−7.15 (m, 2H), 2.46 (s, 6H).

[Ru(bpy)$_2$(L)](PF$_6$)$_2$. L (0.2 g, 0.42 mmol) was dissolved in about 25 mL of $CHCl_3$, and [(bpy)$_2$RuCl$_2$, 2H$_2$O] (0.0743 g, 0.07 mmol) was added and refluxed for 7 h. Then the reaction mixture was evaporated to dryness under reduced pressure. The red solid was redissolved in water and filtered to remove excess L. The desired product was precipitated with aqueous solution of NH_4PF_6 as [Ru(bpy)$_2$(L)] (PF$_6$)$_2$ and purified by column chromatography on neutral alumina (grade III) using acetonitrile−toluene mixtures (70:40; v/v) as eluent. Anal. Found: C, 53.5; H, 3.6; N, 9.5. Calcd: C, 53.39; H, 3.59; N, 9.58. ^{1}H NMR (CD_3CN): δ 8.51−7.19 (calcd 36 H, obsd 35.6 H), 2.50 (s, 3H), 2.38 (s, 3H). MS: molecular ion peak at m/z 1025.

[Ru(bpy)$_2$(L-4DQ)](PF$_6$)$_4$ (L-4DQ = 1-[2-(4′-Methyl-2,2′-bipyrid-4-yl)ethenyl]-4-[2-(4′-methyl-*N*,*N*′-tetramethylene-2,2′-bipyrid-4-yl)ethenyl)]benzene. [Ru(bpy)$_2$(L-4DQ)](PF$_6$)$_4$ was synthesized by the reaction of [Ru(bpy)$_2$(L)](PF$_6$)$_2$ (0.033 g, 28 μmol) and 1,4-dibromobutane (0.0061 g, 28 μmol) in acetonitrile−toluene (3:1, v/v). The reaction mixture was refluxed for 2 days and then dried in vacuo. The crude product was redissolved in acetonitrile, and excess NH_4PF_6 was added. The mixture was stirred for 15 min at room temperature and dried in vacuo. Excess NH_4PF_6 was removed in aqueous layer by solvent extraction. The CH_2Cl_2 layer was dried, and the product was purified by column chromatography on neutral alumina (grade III) using acetonitrile−toluene mixtures (70:30; v/v) as eluent. Anal. Found: C, 44.1; H, 3.5; N, 7.2. Calcd: C, 44.3; H, 3.30; N, 7.37. ^{1}H NMR (CD_3CN): δ 8.51−7.33 (calcd 36H, obsd 36.2H), 2.50 (s, 3H), 2.38 (s, 3H), 1.21 (s, 4H), 0.85 (s, 4H).

C$_4$H$_8$Br$_2$−Y. A mixture of activated zeoliteY (1.0 g) and 1,4-dibromobutane (0.117 mL, 1.0 mmol) in dried *n*-hexane was stirred overnight. Then this zeolite was washed thoroughly with *n*-hexane.

[Ru(bpy)$_2$(L-4DQ)]$^{4+}$−Y. This was prepared by the reaction of [Ru(bpy)$_2$(L)](PF6)$_2$ (0.0059 g, 5 μmol) and C$_4$H$_8$Br$_2$–Y (1.0 g). Reaction was performed in acetonitrile−toluene mixed (3:1; v/v)

(10) Vitale, M.; Castagnola, N. B.; Ortins, N. J.; Brooke, J. A.; Vaidyalingam, A.; Dutta, P. K. *J. Phys. Chem. B* **1999**, *103*, 2408.
(11) Borja, M.; Dutta, P. K. *Nature* **1993**, *362*, 43.
(12) Sykora, M.; Kincaid, J. R. *Nature* **1997**, *387*, 162.
(13) Yong, S. P.; Lee, E. J.; Chun, Y. S.; Yoon, Y. D.; Yoon, K. B. *J. Am. Chem. Soc*. **2002**, *124*, 7123.
(14) Krueger, J. S.; Mayer, J. E.; Mallouk, T. E. *J. Am. Chem. Soc*. **1988**, *110*, 8232.
(15) Li, Z.; Mallouk, T. E. *J. Phys. Chem*. **1987**, *91*, 643.
(16) Shaw, J. R., Webb, R. T.; Schmehl, R. H. *J. Am. Chem. Soc.* **1990**, *112*, 1117.
(17) Strouse, G. F.; Schoonover, J. R.; Duesing, R.; Boyde, S.; Jones, W. E., Jr.; Meyer, T. J. *Inorg. Chem*. **1995**, *34*, 473−487.
(18) Homer, R. F.; Tomilson, T. E. *J. Chem. Soc.* **1960**, 2498.

Scheme 1. Synthesis of $[Ru(bpy)2(L\text{-}4DQ)]^{4+}-Y$

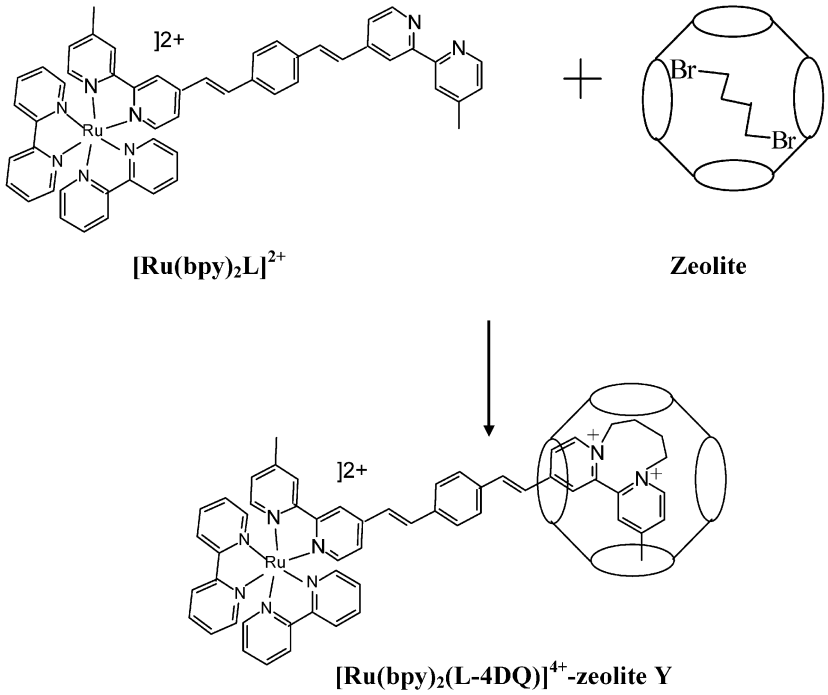

solvent medium. The reaction mixture was refluxed for 3 days followed by extensive washing with acetonitrile. The washing was continued until the solvent was free from the red color of Ru(II)−polypyridyl complex. Then unreacted dihalide was removed by Soxhlet extraction using $CHCl_3$ as a solvent (for about 7 days). The resulting solid was washed thoroughly with 0.5 M NaCl at room temperature followed by sonication at 55 °C with 0.5 M NaCl to remove any Ru(II) complex held to the zeolite surface. Finally, the solid was washed with distilled water to remove excess NaCl.

Electrochemistry. All electrochemistry measurements were carried out with a Princeton Applied Research model 273 potentiostat, using a conventional three-electrode cell assembly. A freshly polished platinium disk electrode (2 mm diameter, CH Instruments) as a working electrode, platinium wire electrode as a counter electrode, and a Ag−AgCl reference electrode were used. Potentials are quoted vs the ferrocene−ferrocenium (Fc/Fc^+) couple since ferrocene was used as an internal standard. Electrochemical measurements were performed using acetonitrile as solvent and 0.10 M tetrabutylammonium hexafluorophosphate ($[Bu^t]_4NPF_6$) as supporting electrolyte.

Photolysis. The light source was a Xenon arc lamp equipped with a water filter, a 420 nm cutoff filter, and a mirror that reflects radiation in the range of 420−650 nm. The power of the radiation incident on the substrate side of the cell was measured by a Coherent 210 power meter and found to be 250 mW/cm^2. Spectral change associated with irradiation of this sample was monitored with a diffuse reflectance UV−vis spectrophotometer (Shimadzu, UV-2501PC with a ISR-2200 integrating sphere attachment).

$[Ru(bpy)_2(L\text{-}4DQ)]^{4+}-Y$ was ion-exchanged with MV^{2+} to produce $[Ru(bpy)_2(L\text{-}4DQ)]^{4+}-MV^{2+}-Y$. Typically 50 mg of $[Ru(bpy)_2(L\text{-}4DQ)]^{4+}-Y$ was ion-exchanged twice with a 0.1 M solution of MV^{2+} overnight and dried under vacuum for 48 h. This $[Ru(bpy)_2(L\text{-}4DQ)]^{4+}-MV^{2+}-Y$ pellet was placed in an anaerobic diffuse reflectance cell in a drybox and exposed to the ambient light. Then the spectral response was monitored using a diffuse reflectance UV−vis spectrophotometer. For suspension photolysis, 50 mg of $[Ru(bpy)_2(L\text{-}4DQ)]^{4+}-Y$ was ion-exchanged twice with a 0.1 M solution of *N*,*N*′-trimethylene-2,2′-bipyridinium ions ($3DQ^{2+}$) for 18 h. $[Ru(bpy)_2(L\text{-}4DQ)]^{4+}-3DQ^{2+}-Y$ powder, thus formed, was air-dried, 0.01 g was placed with 0.01 g of PVS in an NMR tube, and 0.5 mL of degassed distilled water was added. A freeze−pump−thaw cycle was repeated three times to deoxygenate the sample completely. Then this tube was sealed and photolyzed. Spectral change of the solution associated with photolysis was monitored with UV−vis spectrophotometer.

Results

A. Synthesis and Physicochemical Properties. $[Ru(bpy)_2(L)](PF_6)_2$ and $[Ru(bpy)_2(L\text{-}4DQ)](PF_6)_4$. Ligand L and $[Ru(bpy)_2(L)](PF_6)_2$ were prepared by following methods described in the literature with slight modifications.[16] For $[Ru(bpy)_2(L)](PF_6)_2$, $Ru(bpy)_2Cl_2$ was reacted with excess L in $CHCl_3$ rather than ethanol or ethanol−water mixtures. To minimize the possibility of formation of the binuclear Ru(II) complexes, L was used in large excess compared to the $Ru(bpy)_2Cl_2$. $[Ru(bpy)_2(L\text{-}4DQ)](PF_6)_4$ was synthesized by reacting equimolar amounts of $[Ru(bpy)_2(L)](PF_6)_2$ and 1,4-dibromobutane (4DQ being defined as *N*,*N*′-tetramethylene-2,2′-bipyridinium). Analytical and spectroscopic data recorded for these compounds were in agreement with the proposed structures.

$[Ru(bpy)_2(L\text{-}4DQ)]^{4+}-Y$. Loading of 1,4-dibromobutane in zeolite Y during impregnation was restricted to 0.8 mol equiv/supercage. The halide-loaded zeolite was reacted with $[Ru(bpy)_2(L)](PF_6)_2$ for the synthesis of $[Ru(bpy)_2(L\text{-}4DQ)]^{4+}-Y$, as shown in Scheme 1. To confirm that the surface complex was indeed being formed, the zeolite was dissolved in dilute hydrofluoric acid and the complex extracted in CH_2Cl_2 layer. ^1H NMR and UV−vis absorption spectra matched with those of the presynthesized $[Ru(bpy)_2(L\text{-}4DQ)]^{4+}$ sample.

Table 1. Electrochemical Data for Ruthenium(II) Polypyridal Complexes

	$E_{1/2}$,[b] V				
compds[a]	$Ru^{0/-}$	$Ru^{+/0}$	Ru^{2+}/Ru^{+}	L (L-4DQ)	$Ru^{3+/2+}$
$[Ru(bpy)_3]^{2+}$	−2.178	−1.93	−1.74		0.89
$[Ru(bpy)_2(L)]^{2+}$		−2.13	−1.87	−1.66	0.84
$[(bpy)_2Ru(L\text{-}4DQ)]^{4+}$		−2.27	−1.87	−1.36	0.85

[a] As PF_6^- salts. [b]All potential values are quoted vs the Fc^+/Fc couple in CH_3CN solution with 0.1 M $(TBA)PF_6$ as supporting electrolyte; scan rate = 100 mV s^{-1}.

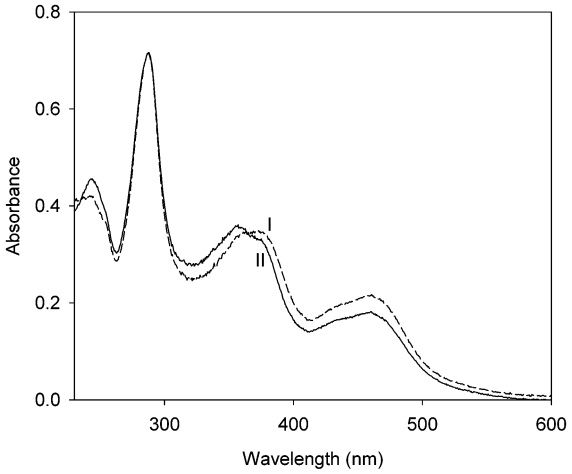

Figure 1. Absorption spectra of a solution of I, $Ru(bpy)_2(L)(PF_6)_2$, and II, $Ru(bpy)_2(L\text{-}4DQ)(PF_6)_4$, in CH_3CN (concentration 8.6 μM).

B. Electrochemistry. Electrochemical properties of the ruthenium complexes were studied by cyclic voltammetry, and the data are shown in Table 1. For $[Ru(bpy)_2(L)]^{2+}$, the redox couple at 0.84 V is due to a Ru(II/III)-based redox process while three ligand-based redox processes appear at −1.66, −1.87, and −2.13 V. The redox couple at −1.66 V is assigned to the $[L/L^{\bullet-}]$-redox couple. For $[Ru(bpy)_2(L\text{-}4DQ)]^{4+}$ the oxidation wave due to Ru(II)/Ru(III) was at 0.85 V and three ligand-based reduction waves at −1.36, −1.87, and −2.27V were observed. The redox wave at −1.36 V is assigned to a $[(L\text{-}4DQ)^{2+}/(L\text{-}4DQ)^{\bullet+}]$-based redox process. The cyclic voltammograms were found to be quasireversible, especially at lower scan rates. This is due to the tendency of the olefinic bpy ligands to form a polymeric film on the working Pt-electrode surface due to reductive electropolymerization, a process that has been reported for Ru(II) diimine complexes having olefinic moieties.[16,19]

C. Optical Spectroscopic Studies of $[Ru(bpy)_2(L)]^{2+}$, $[Ru(bpy)_2(L\text{-}4DQ)]^{4+}$, and $[Ru(bpy)_2(L\text{-}4DQ)]^{4+}$−Y. Ligand L has an absorption maximum at 356 nm with strong emission at 420 nm, as expected from previous reports.[16] Absorption spectra of $[Ru(bpy)_2(L)](PF_6)_2$ and $[Ru(bpy)_2(L\text{-}4DQ)](PF_6)_4$ in CH_3CN are shown in Figure 1. The intraligand ($L/L\text{-}4DQ^{2+}$-based $\pi-\pi^*$) transitions for $[Ru(bpy)_2(L)]^{2+}$ and $[Ru(bpy)_2(L\text{-}4DQ)]^{4+}$ are peaked at 370 and 359 nm, respectively, whereas the metal-to-ligand charge-transfer ($Ru_{d\pi} \rightarrow L_{\pi^*}/L\text{-}DQ^{2+}{}_{\pi^*}$ and bpy-based MLCT) transitions appear at ∼460 nm.

(19) Murray, R. W. *Acc. Chem. Res.* **1980**, *13*, 135.

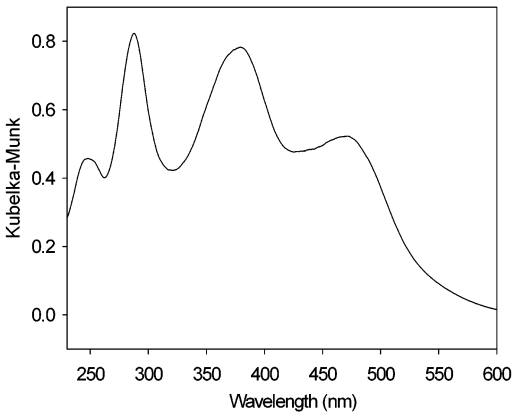

Figure 2. Diffuse reflectance spectrum of $[Ru(bpy)_2(L\text{-}4DQ)]^{4+}$−zeolite Y.

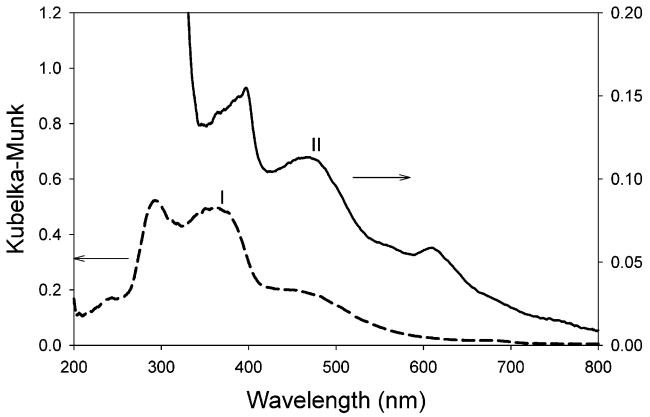

Figure 3. Diffuse reflectance spectra of $[Ru(bpy)_2(L\text{-}4DQ)]^{4+-}$zeolite Y upon ion exchange with MV^{2+} and exposure to the ambient light: I, before MV^{2+} ion exchange; II, after ion exchange with MV^{2+} and exposure to room light.

The diffuse reflectance spectrum for $[Ru(bpy)_2(L\text{-}4DQ)]^{4+}$−Y is presented in Figure 2 and shows an intraligand transition at 370 nm and MLCT band at 470 nm.The emission spectra of $[Ru(bpy)_2(L)]$ and $[Ru(bpy)_2(L\text{-}4DQ)]^{4+}$ in solution show a weak band at 700 nm. The loading level of $[Ru(bpy)_2(L\text{-}4DQ)]^{4+}$ on zeolite Y was determined to be 1.0×10^{-6} mol/g of zeolite Y from elemental analysis, which is consistent with approximate monolayer coverage of zeolite external surface.[15]

D. Photolysis. A solid sample of $[Ru(bpy)_2(L\text{-}4DQ)]^{4+}$−Y ion-exchanged with MV^{2+} upon exposure to ambient light in an anaerobic environment exhibited new bands at 390 and 605 nm, as shown in Figure 3. Further, these spectral changes disappeared when the zeolite sample was subsequently exposed to O_2. These observations are consistent with formation of the $MV^{\bullet+}$ radical.

$Ru(bpy)_2(L\text{-}4DQ)^{4+}$−Y ion-exchanged with $3DQ^{2+}$ was dispersed in a PVS solution and irradiated with visible light. A growth in bands at 390 and 605 nm signifying the formation of $PVS^{\bullet-}$ radical in solution was noted, as shown in the insert of Figure 4. The formation of the viologen radical as measured by the absorbance at 390 nm for two zeolite samples $[Ru(bpy)_2(L\text{-}4DQ)]^{4+}-3DQ^{2+}-Y$ and $[Ru(bpy)_2(L\text{-}4DQ)]^{4+}-Na-Y$ are contrasted in Figure 4. The data show that the growth of $PVS^{\bullet-}$ is considerably accelerated with intrazeolitic $3DQ^{2+}$. After 3 h of photolysis,

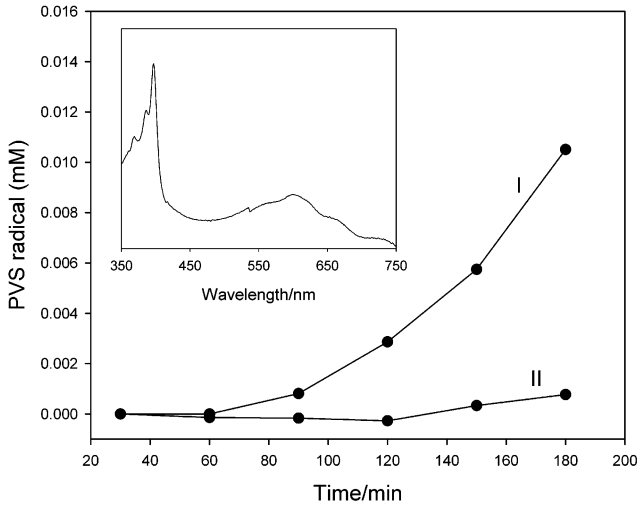

Figure 4. Growth of $PVS^{\bullet-}$ during photolysis of I, $[Ru(bpy)_2(L\text{-}4DQ)^{4+}]-3DQ^{2+}-$zeolite Y, and II, $[Ru(bpy)_2(L\text{-}4DQ)^{4+}]-Na^{+}-Y$, in aqueous solution of 0.01 M PVS (inset shows the spectrum after 180 min of illumination for I).

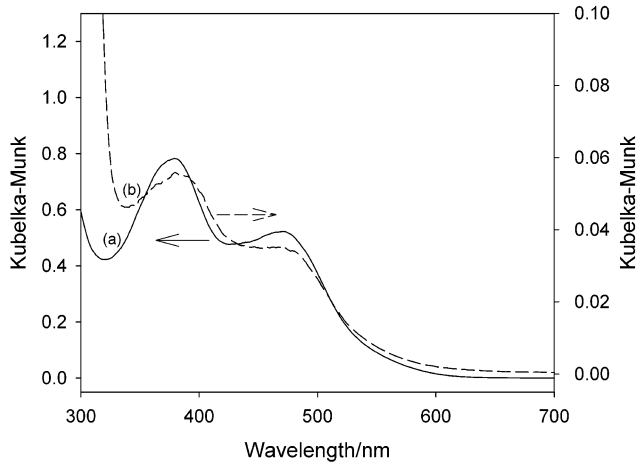

Figure 5. Diffuse reflectance spectra of $[Ru(bpy)_2(L\text{-}4DQ)]^{4+}-$zeolite Y: (a) before photolysis; (b) after photolysis for 180 min.

12 nmol of $PVS^{\bullet-}$ was formed, though the amount of the ruthenium complex on the zeolite was 10 nmol. The yield of $PVS^{\bullet-}$ could be increased further with photolysis time, as is obvious from the slope of $PVS^{\bullet-}$ generation in Figure 4.

After 180 min of photolysis, the solution and zeolite were recovered. Figure 5b shows the diffuse reflectance of the zeolite and is compared to a sample before photolysis (Figure 5a, same as Figure 2). The increase in intensity below 320 nm for the photolyzed sample is due to the presence of intrazeolitic $3DQ^{2+}$, which absorbs at 290 nm. The MLCT and intraligand band positions and relative intensities (due to the Ru complex) of the photolyzed and unphotolyzed sample are similar, indicating that the tethered Ru complex is present on the zeolite after 180 min of photolysis (the differences in absolute intensities are because of the sample size, about 100 mg before photolysis and 5 mg for the photolyzed sample). The stability of the $[Ru(bpy)_2(L\text{-}4DQ)]^{4+}-Y$ system is also consistent with the fact that if the photolysis was continued beyond 180 min, $PVS^{\bullet-}$ continued to grow.

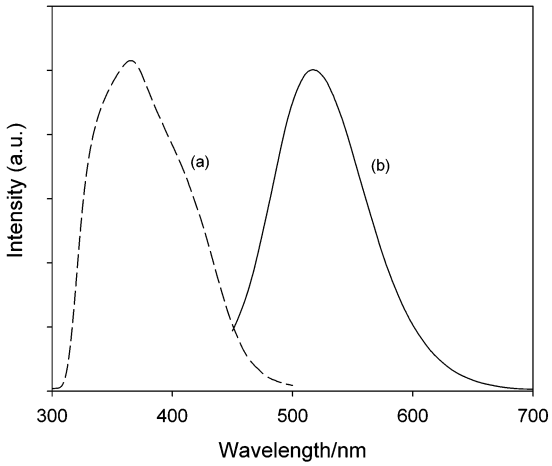

Figure 6. (a) Excitation (monitored at 530 nm) and (b) emission (λ_{exc} = 390 nm) spectra of the solution recovered after 180 min of photolysis.

Several experiments were done with the solution recovered from the photolysis sample. Figure 6 shows the excitation (measured at 530 nm) and emission spectrum (λ_{max} = 530 nm) of the solution. A new species was being created during photolysis with characteristic absorption and emission maximum at 390 and 530 nm. The photolyzed solution was also tested to examine if it had any sacrificial electron donor properties for photolysis with $Ru(bpy)_3^{2+}$ and viologen, and the result was found to be negative. This experiment also confirmed that if any of the zeolite-tethered $[Ru(bpy)_2(L\text{-}4DQ)]^{4+}$ complex was decomposing, then such soluble species did not have the ability to generate $PVS^{\bullet-}$ in solution.

Discussion

$[Ru(bpy)_2(L\text{-}4DQ)]^{4+}-Y$ was synthesized by reacting a pendant bpy unit of $[Ru(bpy)_2(L\text{-}4DQ)]^{4+}$ with 1,4-dibromobutane adsorbed in zeolite supercage. The strategy for surface encapsulation of the Ru complex as outlined in Scheme 1 exploited two features of zeolites. First, the size of the bipyridine moiety on L can readily penetrate through the 7 Å supercage window. Molecular modeling studies show that once the methylated bpy is quaternized by the tetramethylene group, this end gets entrapped in the zeolite. The positive charge on the N's are readily balanced by the zeolite framework. The encapsulation is evident because ion exchange of the derivatized zeolite does not release the $[Ru(bpy)_2\ (L\text{-}4DQ)]^{4+}$ complex. Second, ion exchange leads to a more purified sample, since other Ru polypyridyl complexes adsorbed on the surface are removed. Confirmation of the formation of the surface complex was obtained by dissolution of the zeolite and examining the extract.

The reduction potentials for coordinated L (−1.66 V) and L-4DQ (−1.36 V) are lower than that of coordinated bpy (−1.87 V) groups, reflecting the fact that the conjugated ligands are more easily reduced. The change of ∼300 mV toward positive potentials upon quaternization of the bipyridine moiety of L is consistent with the better electron-withdrawing properties of the bipyridinium (diquat) ion.

Compared to the reduction potential reported for $[(dmb)_2RuL]^{2+}$ (dmb = 4,4′-dimethyl-2,2′-bipyridine),[16] the reduction potential of $[(bpy)_2RuL]^{2+}$ is shifted to more negative values by about ~70 mV, because of the electron-donating properties of the methyl groups. Studies of covalently linked bipyridinium units using saturated spacers show reduction of the attached bipyridinium units,[20−22] unlike what we observe for L-4DQ, where only one reduction wave is observed due to the whole ligand, since it is a single conjugated unit.

There is a blue shift of 10 nm in the intraligand band upon changing from L to L-4DQ that is due to disruption in the conjugation, since the tetramethylene group on the DQ forces the pyridine rings to become become nonplanar.[23] The MLCT band for $[Ru(bpy)_2(L)]^{2+}$ and $Ru(bpy)_2(L\text{-}4DQ)]^{4+}$ are red-shifted by 10 nm compared to $Ru(bpy)_3^{2+}$, suggesting that the MLCT absorption band with L and L-4DQ as ligands involves contributions from the π^* orbital of these conjugated ligands. In the excited state, the electron is therefore expected to be delocalized on L (L-4DQ) rather than the bipyridyl ligand.

The emission maxima of Ru complexes with L and L-4DQ are considerably red-shifted (700 nm) as compared to bipyridyl complexes (620 nm) and with weak emission intensities. For $[Ru(dmb)_2(L)]$, the low quantum yield has been related to lowered intersystem crossing efficiencies to the emitting ^{3}MLCT state.[16]

For polypyridyl ruthenium complexes in solution (e.g., $Ru(bpy)_3^{2+}$), photoexcitation leads to electron localization on a single coordinated bpy ligand.[24] Elliott and co-workers have studied ligands with diquat (*N*,*N*′-diquaternary-2,2′-bipyridinium ions) connected to ligated bipyridyl via saturated spacers and found that the ^{3}MLCT emission is quenched by intramolecular electron transfer from electrons on bpy ligand to the bipyridinium (diquat) moiety.[20] In the present case, because the diquat is connected to the ligated bpy through a conjugated spacer, the electron in the MLCT state is localized on this ligand. Electron-transfer quenching of $[(dmb)_2Ru(L)]^{2+}$ by methyl viologen has been reported.[16] In the present study, intrazeolitic electron transfer from $[(bpy)_2Ru(L\text{-}4DQ)]^{4+}$ to MV^{2+} and $3DQ^{2+}$ is reported.

For calculating the driving force for electron transfer from $[(bpy)_2Ru(L\text{-}4DQ)]^{2+*}$ to viologens in neighboring zeolite cages, it is necessary to estimate the $Ru^{2+*/3+}$ potential. This information can be obtained from the $Ru^{3+/2+}$ potential obtained from cyclic voltammetry (Table 1, 1.22 V vs SHE) and the onset of the emission band.[20] We estimate the onset of the 700 nm emission to be at ~650 nm (~1.9 eV), thereby obtaining a value of −0.68 for the $Ru^{2+*/3+}$ couple. For the two bipyridiniums of interest, MV^{2+} and 3-DQ^{2+}, the driving force for forward electron transfer from photoexcited $[(bpy)_2Ru(L\text{-}4DQ))]^{4+}$ is calculated to be 0.28 and 0.16 V, respectively.

The long-lived $MV^{\bullet+}$ radical that is formed upon illumination of $[Ru(bpy)_2(L\text{-}4DQ)]^{4+}-MV^{2+}-$zeolite is consistent with previous observations, where electron hopping between MV^{2+} within the zeolite lends to propagation of charge away from the Ru center.[10−13] The photolysis studies on the $[Ru(bpy)_2(L\text{-}4DQ)]^{4+}-3DQ^{2+}-$zeolite dispersed in a solution containing PVS showed that, in the presence of $3DQ^{2+}$ in the zeolite, the amount of $PVS^{\bullet-}$ was at least a factor of 10 higher after 180 min of photolysis. The yield of $PVS^{\bullet-}$ after 180 min of photolysis is 12 nmol, which is greater than the amount of Ru complex on the surface of the zeolite (10 nmol) and can be increased further with photolysis time. We believe that the initial period (first 30 min) of slow growth of $PVS^{\bullet-}$ in Figure 4 is due to the residual oxygen in the cell.

On the basis of these data, there are three questions that need to be answered to provide a satisfactory mechanism for the permanent generation of $PVS^{\bullet-}$ in solution. First, why is formation of $PVS^{\bullet-}$ promoted by the presence of intrazeolitic $3DQ^{2+}$? Second, what is the source of electrons for making $PVS^{\bullet-}$? Third, since the yield of $PVS^{\bullet-}$ readily exceeds the surface of the Ru complex, what species must be responsible for regeneration of Ru(II) from Ru(III)? The solution recovered after photolysis has no sacrificial electron donor properties indicating that photodecomposed products are not responsible for formation of $PVS^{\bullet-}$. Spectroscopic data (Figure 5) indicate that the tethered Ru complex on the zeolite survives the photolysis and can be continued for $PVS^{\bullet-}$ generation.

The free-radical-induced oxidation products of methyl viologen have been studied and reported to be pyridones.[25] These ketones are characterized by strong fluorescence. In particular, two strongly fluorescing keto products: 1′,2′-dihydro-l,1′-dimethyl-2′-oxo-4,4′-bipyridinium cation (designated as "2-one") and 3,4-dihydro-1,1′-dimethyl-3-oxo-4,4′-bipyridinium cation (designated as "3-one") have been identified. The 2-one is proposed to form from the adduct by radical−radical disproportionation reactions, whereas the 3-one forms by oxidation of the adduct with oxygen. The species 2-one fluoresces at ~516 nm, with absorption bands at 222, 260, and 347 nm. The 3-one fluoresces at ~528 nm and has absorption bands at 236 and 390 nm. The data in Figure 6 suggest that, in the solution recovered after photolysis, a species with characteristic spectral properties of the 3-one is present, and its source must be the oxidationof PVS in solution. The question that arises is what species oxidizes PVS to the pyridones?

In aqueous solution at neutral pH, the half-life for $Ru(bpy)_3^{3+}$ is of the order of 200 s in the dark and is considerably faster in the presence of visible light.[26] Il-

(20) Cooley, L. F.; Headford, C. E. L.; Elliott, M.; Kelly, D. F. *Am. Chem. Soc.* **1988**, *110*, 6673−6682.
(21) Lomoth, R.; Haupl, T.; Jahansson, O.; Hammarstrom, L. *Chem.—Eur. J.* **2002**, *8*, 102.
(22) Macatangay, A.; Zheng, G. Y.; Rillema, D. P.; Jackman, D. C.; Merkert, J. W. *Inorg. Chem.* **1996**, *35*, 6823−6831.
(23) Amouyal, E.; Zidler, B. *Isr. J. Chem.* **1982**, *22*, 117.
(24) McClanahan, S. F.; Dallinger, R. F.; Holler, F. J.; Kincaid, J. R. *J. Am. Chem. Soc.* **1985**, *107*, 4853−4860.
(25) (a) Solar, S.; Solar, W.; Getoff, N. *J. Chem. Soc., Faraday Trans. 1* **1985**, *81*, 1101. (b) Bahnemann, D. W.; Fischer, C.-H.; Janata, E.; Henglein, A. *J. Chem. Soc., Faraday Trans. 1* **1987**, *83*, 2559.
(26) Ghosh, P. K.; Brunschwig, B. S.; Chou, M.; Creutz, C. Sutin, N. *J. Am. Chem. Soc.* **1984**, *105*, 4832.

Scheme 2. Photoelectron-Transfer Scheme of $[Ru(bpy)_2(L\text{-}4DQ)]^{4+}-3DQ^{2+}-$Zeolite Y in Aqueous Solution of PVS

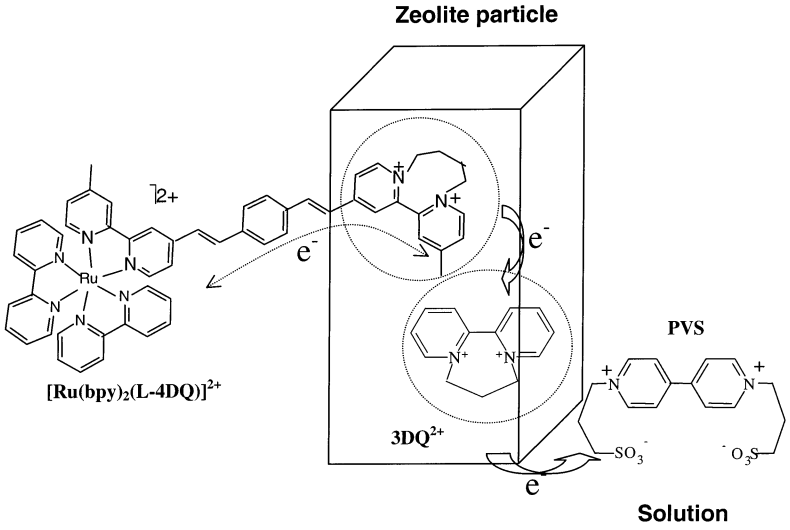

lumination within the ligand to metal charge-transfer band of $Ru(bpy)_3^{3+}$ increases the nucleophilicity of the bpy ligand and thereby promotes the attack by water. In earlier studies,[27,28] we concluded that the covalent hydrates and hydroxylated species of the ruthenium complex formed by the attack of water on $Ru(bpy)_3^{3+}$ oxidize methyl viologen to pyridones and regenerate $Ru(bpy)_3^{2+}$. We propose that, in the $[Ru(bpy)_2(L\text{-}4DQ)]^{4+}-3DQ^{2+}-$zeolite sample, photoexcitation leads to electron transfer from the tethered Ru complex to intrazeolitic $3DQ^{2+}$. Several studies in zeolites have demonstrated that if the bipyridinium ions in zeolite are well packed, then the electron can migrate through the zeolite by self-exchange,[10−13] and this is the purpose DQ^{2+} serves. Such a process will lead to the formation of Ru(III) on the zeolite surface, which in the presence of light and water will lead to rapid adduct formation that can react with PVS in solution to form the pyridones and regenerating Ru(II). The electron on the $3DQ^{2+/+}$ can migrate through the zeolite and upon coming to the surface of the zeolite is vectorially transferred (because of the difference in reduction potentials) to PVS in solution forming $PVS^{\bullet-}$, a feature that has also been reported by other groups.[12,13] These ideas are expressed in Scheme 2 and represented by the following equations:

$$Ru^{II}-\text{zeolite} \xrightarrow{h\nu} Ru^{II*}-\text{zeolite}$$

$$Ru^{II*}-\text{zeolite} + 3DQ^{2+}-\text{zeolite} \rightarrow Ru^{3+}-\text{zeolite} + 3DQ^{\bullet+}-\text{zeolite}$$

$$Ru^{3+}-\text{zeolite} + H_2O \xrightarrow{h\nu} Ru^{3+}(OH_2)-\text{zeolite}$$

$$Ru^{3+}(OH_2)-\text{zeolite} + PVS \rightarrow Ru^{2+}-\text{zeolite} + \text{pyridones}$$

$$3DQ^{\bullet+}-\text{zeolite} + PVS(\text{soln}) \rightarrow 3DQ^{2+}-\text{zeolite} + PVS^{\bullet-}(\text{soln})$$

In the scheme above, the $Ru^{3+}(OH_2)-$zeolite represents the complex formed by water attack on the Ru(III) complex and its actual form is more complicated than the representation.[26−28] The reason the electron at the interface (on $3DQ^{2+}$) does not recombine with the ruthenium complex is because Ru(III) has reacted with water and PVS and regenerated as Ru(II). Thus, both water and PVS are necessary to regenerate Ru(II). PVS also plays a second role as the electron acceptor from $DQ^{\bullet+}$ in the zeolite. Eventually, the formation of $PVS^{\bullet-}$ will stop when all the PVS is converted to the pyridone, but since we have a 2500-fold excess of PVS over ruthenium, such a situation is not reached within the times for which we have photolyzed the samples.

Water attack on the photogenerated Ru(III) complex will result in degradative processes and destruction of the Ru complex in the absence of PVS.[26,27] Zeolite-based RuO_2 catalytic systems that can result in O_2 generation are currently being incorporated into the molecular assembly and will assist in regeneration of the Ru(II) complex.[29] Also, in the present system (Scheme 2), there is a sacrifice in photochemical efficiency due to quenching of $[Ru(bpy)_2(L\text{-}4DQ)]^*$ by PVS in solution. Use of a zeolitic membrane that separates the redox species will alleviate this problem and is being investigated.[30]

In conclusion, it is important to note that the zeolite architecture is responsible for the permanent generation of $PVS^{\bullet-}$ in solution by slowing the back electron transfer within the tethered $[Ru(bpy)_2(L\text{-}4DQ)]$ complex and making possible the electron transfer to the intrazeolitic $3DQ^{2+}$. The observations in this study are consistent with the long-lived electron-transfer processes that have been reported in zeolite hosts.[9−13]

(27) Ledney, M.; Dutta, P. K. *J. Am. Chem. Soc.* **1995**, *117*, 7687.
(28) Das, S. K.; Dutta, P. K. *Langmuir* **1998**, *14*, 5121.
(29) Das, S. K.; Dutta, P. K. *Microporous Mesoporous Mater.* **1998**, *22*, 475.
(30) Lee, H.; Dutta, P. K. *J. Phys. Chem. B* **2002**, *106*, 11898.

Conclusion

A photoactive Ru(II)−polypyridyl unit has been entrapped on the surface of zeolite Y supercage. Electrochemical and optical studies indicate that upon photoexcitation the MLCT state has the electron delocalized on the ligand that is entrapped within the zeolite. Electron transfer from the photoexcited state to bipyridinium ions within the zeolite was observed. Photolysis of the modified zeolite, $[Ru(bpy)_3(L\text{-}4DQ)^{4+}-Y-3DQ^{2+}-PVS_{soln}]$, produces permanent charge separation through successive electron transfer from the ligand L-4DQ to intrazeolitic $3DQ^{2+}$ and then eventually from $3DQ^{\bullet+}$ to PVS in solution. The regeneration of Ru(II) occurs by a photomediated reaction of water with Ru(III) followed by oxidation of PVS to pyridones.

Acknowledgment. We acknowledge support form The Ohio State University, NASA, and NSF (Grant INT 0096798) and thank Kefa Onchoke for the zeolite modeling data.

IC034216O